Biosensors and Bioelectronics 107 (2018) 17–25

Contents lists available at ScienceDirect

Biosensors and Bioelectronics

journal homepage: www.elsevier.com/locate/bios

Enzymatic fuel cells with an oxygen resistant variant of pyranose-2-oxidase as anode biocatalyst

Samet Şahin[a,b], Thanyaporn Wongnate[c], Litavadee Chuaboon[d], Pimchai Chaiyen[c,d], Eileen Hao Yu[a,*]

[a] School of Chemical Engineering and Advanced Materials, Newcastle University, Newcastle upon Tyne, England, NE1 7RU, UK
[b] Department of Chemical Engineering, Faculty of Engineering, Bilecik Şeyh Edebali University, 11230 Bilecik, Turkey
[c] Department of Biomolecular Science and Engineering, School of Biomolecular Science & Engineering, Vidyasirimedhi Institute of Science and Technology (VISTEC), Wangchan Valley, Rayong 21210, Thailand
[d] Mahidol University, Department of Biochemistry and Center for Excellence in Protein and Enzyme Technology, Faculty of Science, Bangkok 10400 Thailand

ARTICLE INFO

Keywords:
Biosensors
Enzymatic fuel cells
Pyranose-2-oxidase
Glucose oxidase
Ferrocene
Nafion

ABSTRACT

In enzymatic fuel cells (EnFCs), hydrogen peroxide formation is one of the main problems when enzymes, such as, glucose oxidase (GOx) is used due to the conversion of oxygen to hydrogen peroxide in the catalytic reaction. To address this problem, we here report the first demonstration of an EnFC using a variant of pyranose-2-oxidase (P2O-T169G) which has been shown to have low activity towards oxygen. A simple and biocompatible immobilisation approach incorporating multi-walled-carbon nanotubes within ferrocene (Fc)-Nafion film was implemented to construct EnFCs. Successful immobilisation of the enzymes was demonstrated showing 3.2 and 1.7-fold higher current than when P2O-T169G and GOx were used in solution, respectively. P2O-T169G showed 25% higher power output (maximum power density value of 8.45 ± 1.6 μW cm^{-2}) and better stability than GOx in aerated glucose solutions. P2O-T169G maintained > 70% of its initial current whereas GOx lost activity > 90% during the first hour of 12 h operation at 0.15 V (*vs* Ag/Ag^{+}). A different fuel cell configuration using gas-diffusion cathode and carbon paper electrodes were used to improve the power output of the fuel cell to 29.8 ± 6.1 μW cm^{-2}. This study suggests that P2O-T169G with low oxygen activity could be a promising anode biocatalyst for EnFC applications.

1. Introduction

In recent years, development of enzymatic electrodes for bioelectronic applications has attracted many researchers' attention because of their highly efficient catalytic activity for biological reactions (Rasmussen et al., 2016). Enzymatic electrodes are mostly employed in healthcare applications such as biosensors, especially for the detection of glucose (Salek-Maghsoudi et al., 2018), lactate (Rathee et al., 2016), cholesterol (Dey and Raj, 2010) and non-esterified fatty acids (Kang et al., 2014). Enzymatic fuel cells (EnFCs) utilising glucose are another example where enzymatic electrodes have been extensively used to harvest micro-power for implantable and small electronic devices (Yu and Scott, 2010).

Lignocellulosic biomass is the most abundant renewable biological resource available on earth and is a suitable raw material for biofuels and chemicals (Dougherty et al., 2014). EnFCs could be a good alternative to utilise sugars from hydrolysis of lignocellulosic biomass for energy generation, particularly with the safety concerns in aviation travel on Li-battery and alcohol fuel cells used in electronic devices, such as laptops and mobile phones (Kim et al., 2016; Schievano et al., 2016). EnFCs using sugars as fuel for power generation possess advantages with widely available sugar source and non-flammable nature.

Different enzymes and immobilisation approaches for enzyme electrodes have been developed to improve the power output and stability of EnFCs (Rasmussen et al., 2016). One of the most important issues in the development of enzymatic electrodes is the successful and efficient transfer of electrons between enzyme and electrode. A number of different electron transfer mediators have been used to fabricate enzymatic electrodes such as osmium (Os), benzoquinone, poly-vinylferrocene, ferrocene (Fc) and its derivatives (Ivanov et al., 2010). Among all the mediators employed, Fc and its derivatives stand out because of their non-toxicity to human body and their solubility in different solvents such as water and ethanol (Harkness et al., 1993; Stepnicka, 2008).

Several methods have been applied to fabricate Fc integrated enzyme electrodes for biosensors and EnFCs to achieve stable and

* Correspondence to: Newcastle University, School of Chemical Engineering and Advanced Materials, Merz Court, Newcastle upon Tyne, England, NE1 7RU, UK.
E-mail address: eileen.yu@ncl.ac.uk (E.H. Yu).

https://doi.org/10.1016/j.bios.2018.01.065
Received 18 December 2017; Received in revised form 26 January 2018; Accepted 30 January 2018
Available online 01 February 2018

electrochemically active enzyme electrodes (Abdulbari and Basheer, 2017; Saleem et al., 2015; Yang et al., 2003). Coatings of Fc-Nafion films were shown to be promising for the fabrication of long term stable and electrochemically active enzyme electrodes as Nafion is readily permeable to glucose (Dong et al., 1992; Vaillancourt et al., 1999). Although promising results were obtained, fabricated electrodes suffered from several problems such as low electrical conductivity of the films formed, some interferences due to electropolymerization processes and the long-term leaching of both enzyme and mediator. In more recent years, Nafion supported systems was also used for uric acid, dopamine and alcohol biosensors (Chen et al., 2011; Chinnadayyala et al., 2014; Ghosh et al., 2015). However, there is still room for improvement as the properties of these films can be enhanced using novel materials and immobilisation methods.

Carbon nanotubes (CNTs) have been used to enhance the properties of Fc-Nafion films because of their unique properties of biocompatibility and excellent electrical communication it can provide between the enzymes and the electrodes with the integration of electron transfer mediators and polymer matrixes (Dai, 2002; Meredith et al., 2011; Smart et al., 2006; Tran et al., 2011). In particular, non-covalent binding of molecules to the CNTs sidewalls obtaining strong π- π interactions using pyrene and its derivatives provides a wide range of possibilities for enzyme immobilisation (Jönsson-Niedziolka et al., 2010). This approach has been widely used in the field of EnFCs (Güven et al., 2016; Halámková et al., 2012; Krishnan and Armstrong, 2012; MacVittie et al., 2013; Szczupak et al., 2012). High surface area carbon material on the electrode surface can provide successful crosslinking of enzymes and better conductivity using pyrene and/or its derivatives. It has also been reported that dispersions prepared using multi-walled carbon nanotubes (MWCNTs) and Nafion showed promising results for biosensors such as bilirubin and glucose determination (Filik et al., 2015; Mani et al., 2013).

Glucose oxidase (GOx) is one of the most widely used enzyme in EnFCs and has many advantages due to its well-known structure as well as inexpensive, stable and practical use (Heller, 2004; Willner et al., 2009; Wilson and Turner, 1992). It has, however, significant drawbacks including restricted turnover rates for glucose and high turnover rates for oxygen (Zafar et al., 2010). Pyranose-2-oxidase (P2O), on the other hand, is a wood degrading enzyme and has become popular due to its excellent reactivity with alternative electron acceptors for a range of sugar substrates (Odaci et al., 2008; Tasca et al., 2007). As P2O has high specificity toward aldopyranose sugar, it can be applied for detection of D-glucose or 1,5-anhydroglucitol, an analogue of D-glucose found in serum of diabetes patient (Yabuuchi et al., 1989). Unlike GOx, P2O can use both α, and β-D-glucose as substrates, therefore, P2O can generate more redox output from glucose oxidation than GOx which can result higher power outputs in EnFCs (Tasca et al., 2007).

There are several studies toward the immobilisation of P2O for biosensor applications, wherein the co-immobilisation of P2O with peroxidase on a carbon paste electrode was one of the earliest reports (Lidén et al., 1998). A few studies have been reported using P2O with different flexible Os functionalized polymers (Tasca et al., 2007; Timur et al., 2006; Zafar et al., 2010). Although these reports show promising results with Os polymers, there is a concern about their use in implantable devices. Os compounds are toxic and not biocompatible, therefore leaching is a serious concern posing a high risk for long term applications (Yu and Scott, 2010). Other studies demonstrate the use of carbon nanotubes (CNTs) and gold nanoparticle-polyaniline/gelatin nanocomposites with P2O enzyme to fabricate biosensors (Odaci et al., 2008; Ozdemir et al., 2010). According to authors' best of knowledge, there are a couple of studies utilising P2O in EnFCs (Kim et al., 2017; Kwon et al., 2014). Researchers employed P2O and GOx in a fuel cell reaching power densities of 40.7 $\mu W\,cm^{-2}$ using an air-breathing platinum cathode (Kwon et al., 2014). In another one, researchers used enzyme precipitate coating method to immobilise P2O at the anode and platinum at the cathode reaching power density values of 53 $\mu W\,cm^{-2}$ (Kim et al., 2017). In both of the studies, researchers did not present a fully enzymatic system and they used electron mediators in solution for oxidation reactions.

In this study, oxygen insensitive variant of P2O (P2O-169G) was used as anode catalyst in a full enzymatic fuel cell and compared with widely used GOx fuel cell. P2O-169G was constructed using semi-rational protein design and reported not to utilise as much oxygen as their wild type form but still retain the advantages of oxidizing sugars of the wild type enzyme (Pitsawong et al., 2010). Mechanistic details underlying how the active site controls oxygen reactivity of P2O have been elucidated by density functional theory, transient kinetics and site-directly mutagenesis to be involved with proton-coupled electron transfer reaction (Wongnate et al., 2014). P2O also showed good oxidation activity for various sugars, not only specific to glucose (Spadiut et al., 2010). This makes it more attractive for EnFC applications with broader fuel sources.

The behaviour of P2O-T169G enzyme in electrochemical systems can provide important information to develop more efficient and stable electrodes. In a previous study, a comparative study testing the electrochemical behaviour and stability of P2O-T169G and GOx enzymes in oxygen saturated solutions was reported (Sahin et al., 2014). We here report the electrochemical performance of P2O-T169G and GOx when immobilised on Fc-MWCNTs modified carbon screen-printed (SPE) and carbon paper electrodes (CPE) using pyrene crosslinking chemistry. The fuel cell performance of the P2O-T169G as an anode biocatalyst was investigated and compared with the results obtained using GOx. Finally, the P2O-T169G fuel cell was tested in an air-breathing enzyme cathode system. The results suggested P2O-T169G with low oxygen activity is a good candidate for EnFCs.

2. Experimental

2.1. Materials

Chemicals used in this study and the details of the electrodes used are summarised in Table S1. P2O-T169G (prepared using site-directed mutagenesis at position Thr169, 0.2 U/mg) was prepared as reported previously (Pitsawong et al., 2010; Wongnate et al., 2011). MWCNTs (inner diameters of 20–50 nm and outer diameters of 70–200 nm) were obtained from Applied Sciences Inc. (Ohio, USA). Perspex cells used for the experiments were made in house.

2.2. Fabrication of enzyme electrodes

The schematic display of the immobilisation process for SPEs is shown in Fig. 1. Briefly, Fc-Nafion-MWCNTs composite was prepared by mixing 1 mg of MWCNTs in 1 mL of 25 mM Fc containing 1 wt% Nafion solution with 90% ethanol at pH 7 under sonication for 3 h using a similar approach reported before by Dong et al. (1992). A solution of Fc-Nafion-MWCNTs was drop coated onto carbon SPEs in small additions with drying time allowed between each step. Then, the dried electrode was placed in a perspex cell and a preconditioning step of 20 cyclic voltammetry (CV) scans at 50 $mV\,s^{-1}$ between − 0.4 V and 0.4 V (*vs* Ag/Ag^{+}) was applied. After the preconditioning step, the electrode was washed with de-ionised water, dried in an oven at 35 °C for 10 min. Immobilisation of the enzymes were performed using a heterobifunctional cross-linker, 1-Pyrenebutyric acid N-hydroxysuccinimide ester (PBSE, 10 mM in dimethylformamide) for 1 h following by incubating activated electrodes with enzyme solutions for 2 h. Since PBSE has an N-hydroxysuccinimide group attached to the acid, it eliminates the extra carbodiimide + ester step in conventional approaches hence resulting in easier fabrication of enzyme electrodes. The electrodes then were rinsed with de-ionised water and/or phosphate buffer solution (PBS) (0.1 M, pH 7) between each step to remove weakly bonded species and tested in 0.1 M PBS at pH 7 without further treatment. Immobilisation in CPEs were also performed using the same procedure.

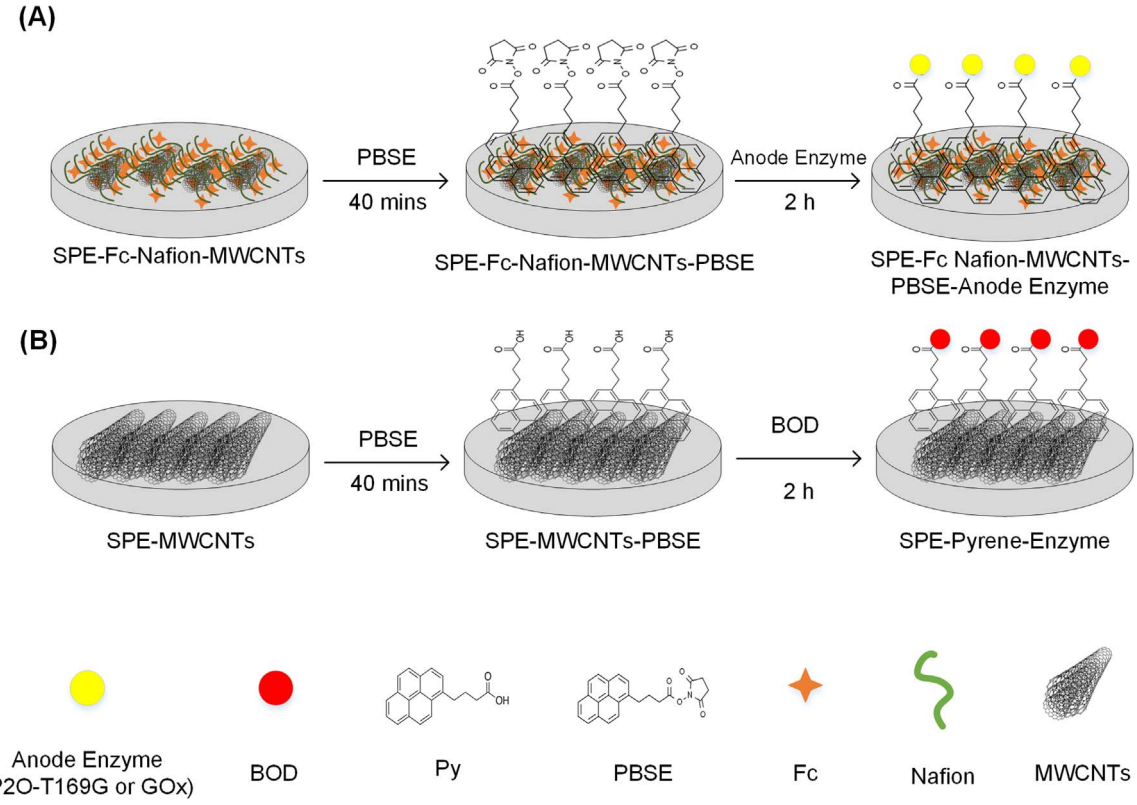

Fig. 1. Schematic representation of (A) anode and (B) cathode preparation.

2.3. Electrochemical characterisation and fuel cell polarisation

2.3.1. Electrochemical characterisation

Electrochemical measurements were carried out using Perspex cells and an Autolab potentiostat-galvanostat (PGSTAT101 by Metrohm Autolab B.V., Netherlands). Prior to the electrochemical tests the solutions were sparged with either air or nitrogen before and between each consecutive glucose additions. Cyclic voltammetry (CV), linear sweep voltammetry (LSV) and chronoamperometry (CA) were carried out in PBS with various glucose concentrations. Stock solutions of glucose were allowed to mutarotate for minimum 24 h before use and were subsequently kept refrigerated at 4 °C. Different glucose concentration was achieved by stepwise addition of glucose stock solution to the cell filled with 0.5 mL PBS. CV experiments were performed at different scan rates from 500 mV s^{-1} to 5 mV s^{-1}, LSV experiments were performed at 1 mV s^{-1} and CA experiments were carried out by applying constant voltage over time and recording the current after consecutive glucose additions in every 10 min. Also, CA under constant nitrogen or air sparging was carried out for stability studies.

2.3.2. Fuel cell polarisation

Two different fuel cell configurations were employed in this study using batch and continuous operating modes. In the first configuration, a glass beaker filled with aerated glucose solution (5.5 mM in 0.1 M PBS at pH 7) was used as fuel cell compartment. P2O-T169G and GOx on the anode and Bilirubin oxidase (BOD) on the cathode at concentrations of 4 mg mL^{-1} was immobilised on SPEs respectively as described in Fig. 1. In the latter configuration, a fuel cell with an air breathing cathode with gas diffusion layer was used on carbon paper. (Supplementary Fig. 1). P2O concentration of 10 mg mL^{-1} on the anode and 4 mg mL^{-1} of BOD on the cathode were immobilised on carbon paper respectively as described in Fig. 1. Electrochemical characterisation of BOD was shown in Supplementary Fig. 8.

Fuel cell polarisation tests were performed using a resistor box (Model: RS-500 (range: 1 Ω-10 MΩ) from Elenco Electronics, Wheeling, US) to apply load and the output voltage was recorded on a computer via data logger (Model: ADC-16 from Pico Technology, Cambridgeshire, UK). The resistance on the fuel cell was changed between 10 MΩ and 1 kΩ and the real-time voltage response was recorded. The current and power of the fuel cell was then calculated using Ohm's Law ($V = I \times R$ and $P = I \times V$). The anode and cathode potentials were also recorded *vs* Ag/AgCl reference electrode (saturated KCl gel filled, 0.197 V vs SHE (Bard et al., 1980)). Stability tests were performed in continuous operation mode using a peristaltic pump (from Watson Marlow, model: 101U/R) to circulate aerated glucose solution (5.5 mM in 0.1 M PBS at pH 7) at a flow rate of 0.3 mL min^{-1}. The voltage recordings and related calculations were performed same as polarisations tests. All the measurements were carried out at room temperature.

3. Results and discussion

3.1. Preparation and optimisation of Fc-Nafion-MWCNTs loading on SPEs

The electrochemical incorporation of a cationic redox coupled (such as Fc) into an anionic perfluorsulfonated polymer (such as Nafion) has been reported previously to construct modified electrodes for electrochemical glucose oxidation (Dong et al., 1992; Vaillancourt et al., 1999). In this study, a new approach for fabricating Fc-Nafion films on carbon SPEs was investigated with the incorporation of MWCNTs in order to improve the electrical conductivity and obtain higher surface area for electron transfer and enzyme immobilisation respectively.

Fig. 2(A) and (B) show the SEM images of bare and Fc-Nafion-MWCNTs modified electrodes. It can be seen that Nafion polymer is wrapped around the MWCNTs and acts as a binder to provide a uniform film on SPE, suggesting that a homogenous dispersion of MWCNTs could be achieved with ethanoic Fc-Nafion solution. Fc can also be seen in the form of micrometric crystals in Fc-Nafion-MWCNTs films (Supplementary Fig. 2(A)). Fig. 2(C) shows the pre-conditioning step of

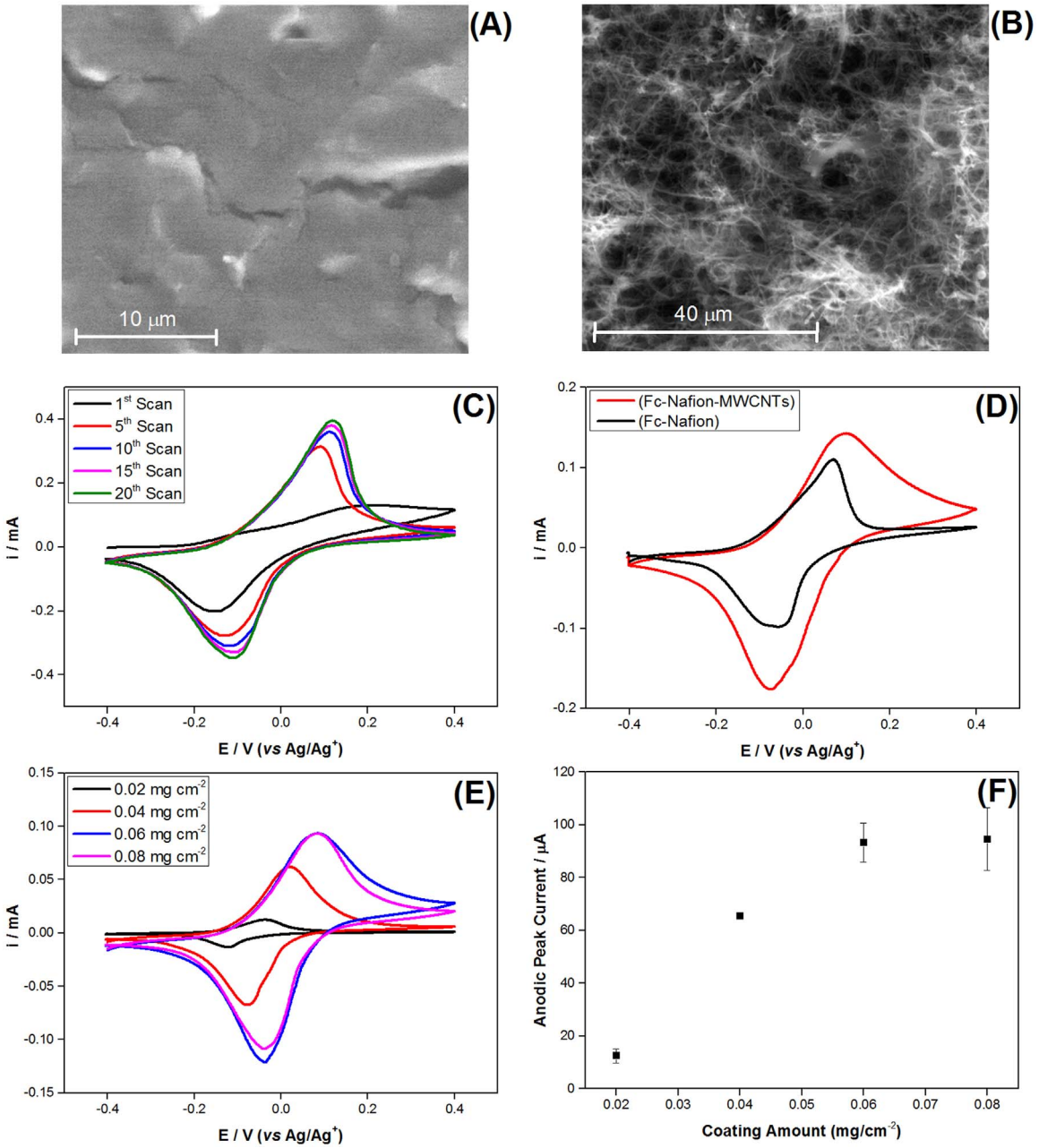

Fig. 2. SEM images of (A) bare SPE and (B) Fc-Nafion-MWCNTs modified SPE. (C) Pre-conditioning step for Fc-Nafion coated SPE, 20 cycles of CV scans applied at 50 mV s^{-1}, FcNafion coating amount = 0.06 mg cm^{-2}. (D) The effect of MWCNTs in the performance of Fc-Nafion modified electrodes tested after pre-conditioning at scan rate of 5 mV s^{-1}. (E) The effect of the different amounts of Fc-Nafion-MWCNTs coated on carbon SPE tested after pre-conditioning at scan rate of 5 mV s^{-1}. (F) Anodic peak current values for different coating amounts derived from Fig. 2(E). All experiments were conducted in 0.1 M PBS at pH 7. Error bars are sample standard deviations (n = 3 samples).

Fc-Nafion modified carbon SPE performed using CV at 50 mV s^{-1} scan rate in 0.1 M PBS at pH 7. The current increased with increasing scan number and become saturated around the 20th cycle. The shape of the anodic peak for the first cycle behaved different than the rest of the scans (no definitive oxidation peak) as the species might be moving into different domains of the Nafion layer during the first cycle. This is similar to studies reported in literature (Dong et al., 1992).

The difference between two pre-conditioned carbon SPEs tested is demonstrated in Fig. 2(D). One of the electrodes was modified with Fc-Nafion mixed with MWCNTs (1 mg mL^{-1}) when the other was modified only with Fc-Nafion. MWCNTs modified film showed higher currents in both anodic and cathodic reactions suggesting more efficient electron transfer from Fc to the electrode due to electrically conductive nature of the nanomaterial. It was also observed that the SEM image of pre-conditioned Fc-Nafion-MWCNTs electrode was clearer compared to non-conditioned electrode (Supplementary Fig. 2(B)). This might be because of the Nafion film structure is changing during the pre-conditioning step by accumulation of Fc. Different film loadings were also applied on carbon SPEs to optimise the coated electrodes. The main purpose of this optimisation was to find the minimum film loading on the electrode with maximum concentration of Fc possible. In doing so, the thickness of the Nafion layer can be minimised and the number of the mediator molecules can be maximized on the electrode for more efficient electron transfer between enzyme and the mediator.

Fig. 2(E) shows the CVs performed to investigate the effect of different Fc-Nafion-MWCNTs coating amounts on the anodic and cathodic reactions as more of the film was loaded onto the electrodes. The peak currents were also presented as a function of film loading (Fig. 2(F)).

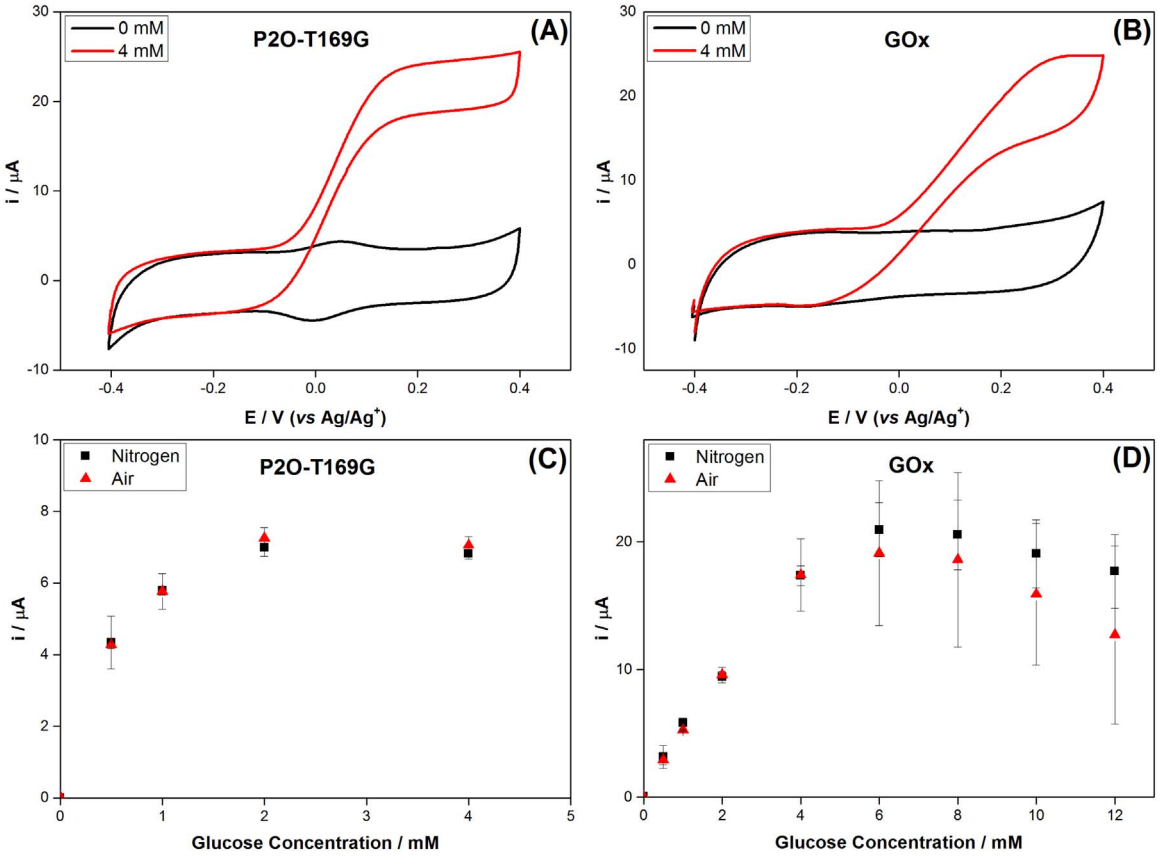

Fig. 3. CV (scan rate: 5 mV s^{-1}) scans of (A) P2O-T169G and (B) GOx immobilised on Fc-Nafion-MWCNTs pre-conditioned carbon SPE. SPEs were tested with 0 mM and 4 mM glucose in nitrogen saturated solutions of 0.1 M PBS at pH 7, electrode model: DRP-C110, surface area: 0.126 cm^2. CA experiment at 0.15 V (*vs* Ag/Ag^+) of (C) P2O-T169G and (D) GOx for various glucose concentrations. Electrode model: DRP-C1110, surface area: 0.059 cm^2. Error bars are sample standard deviations (n = 2 samples).

The current response showed increasing current values until the loading of Fc reached 0.06 mg cm^{-2} and stayed stable even when the loading was increased to 0.08 mg cm^{-2} and the error margin got larger as the film loading was increased. This could be due to excessive loading of the material hence resulting in leaching or instability of the film. The optimum film loading was selected as 0.06 mg cm^{-2} and used as the electrode configuration for enzyme immobilisation procedures.

3.2. Glucose oxidation with P2O-T169G and GOx immobilised on Fc-Nafion-MWCNTs enzyme electrodes

Fig. 3 shows the electrochemical behaviour of P2O-T169G and GOx immobilised on Fc-Nafion-MWCNTs pre-conditioned SPEs using PBSE as demonstrated in Fig. 1. It can be seen from Fig. 3(A) and (B) that the current response of the electrodes without any glucose present in the solution was similar to the typical redox behaviour of Fc in electrochemical systems showing very low activity. Small redox peaks can be seen around 0.05 V and 0 V for oxidation and reduction of Fc, respectively, for P2O-169G immobilised SPE and very little activity around the same voltages for GOx. Peak separation of 50 mV was calculated suggesting a reversible electron transfer mechanism for P2O-T169G (Scholz, 2010). CV data for various glucose concentrations were also presented in Supplementary Fig. 3.

Enzymes demonstrated an increased oxidative current response with increased glucose concentrations and displayed the same onset potential (around − 0.1 V *vs* Ag/Ag^+) in the CV test which is dependent on the activation of the glucose oxidation reaction similar to the results with FcCOOH in solution. This suggests the immobilisation of the enzymes on the electrode surface and electron transfer between the enzyme and electrode *via* Fc mediator are achieved successfully for Fc-Nafion-MWCNTs modified electrodes.

Fig. 3(C) and (D) show the results derived from CA experiments performed at 0.15 V (*vs* Ag/Ag^+) by recording the steady state current after consecutive glucose additions every 10 min under air and nitrogen saturated solution conditions (Raw data is presented in Supplementary Fig. 4). P2O-T169G demonstrated increasing current after each glucose addition up to around 4 mM glucose concentration where GOx showed increasing current up to 6 mM. The performance of the enzymes seemed to be lower than where the FcCOOH was used in the solution (Supplementary Fig. 5(C) and (D)). Although this sort of behaviour can be expected due to the restricted mobility of the entrapped Fc inside Nafion clusters since it is a diffusive mediator and smaller amounts of Fc being present in the immobilised system than in solution. It was calculated that the amount of Fc entrapped on the electrode surface was estimated to be approximately 2.7-fold less than where it was used in the solution experiments (assuming no Fc leaching during the test). Voltammetry experiments also showed that the background current for the system was approximately 6 and 3-fold lower than where FcCOOH was in the solution for P2O-T169G and GOx respectively. The high background current from the solution system was expected due to FcCOOH being in the solution whereas only PBS was used in the experiments for immobilised electrodes.

The K_m values for P2O-T169G and GOx under air saturated solutions were calculated as 0.68 mM and 0.17 mM respectively up to 8 mM glucose concentration range (R^2 = 0.9837 and R^2 = 0.9976 for P2O-T169G and GOx respectively, Lineweaver-Burk plot is presented in Supplementary Fig. 6). I_{max} values for P2O-T169G and GOx were also calculated as 25.2 µA and 36.87 µA, respectively showing higher values than obtained in CA experiments especially for P2O-T169G. Compared to the system where FcCOOH was used in the solution, GOx showed better affinity towards glucose whereas P2O-T169G did not show significant change (Lineweaver-Burk plot is presented in Supplementary

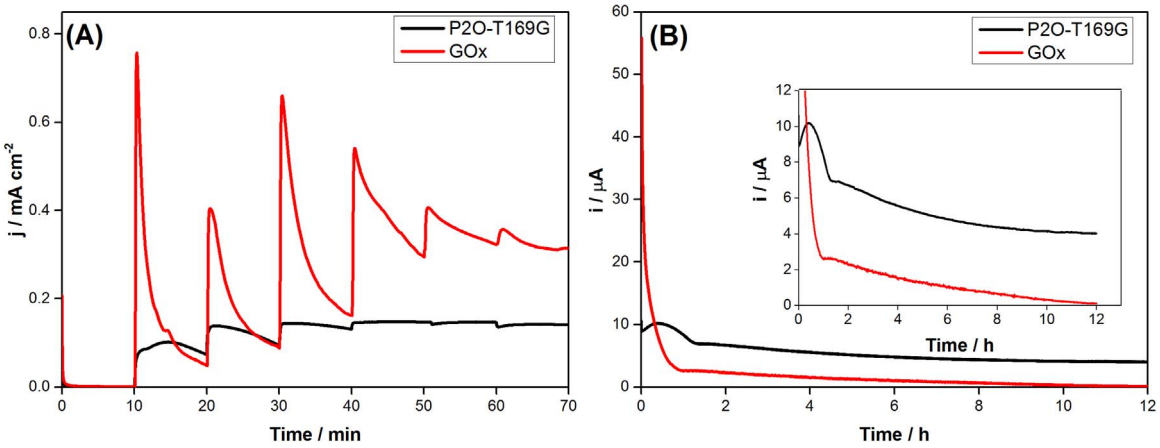

Fig. 4. (A) CA experiments at 0.15 V (*vs* Ag/Ag^+) of various glucose concentrations for P2O-T169G and GOx enzymes immobilised on Fc-Nafion-MWCNTs modified SPEs. SPEs were tested in air saturated solutions of 0.1 M PBS at pH 7. (B) CA experiments at 0.15 V (*vs* Ag/Ag^+) for P2O-T169G and GOx (inset graph: reduced current range for close up view of (B)). SPEs were tested in air saturated solutions of 0.1 M PBS at pH 7 containing 4 mM glucose for 12 h. Electrode model: DRP-C110, surface area: 0.126 cm^2.

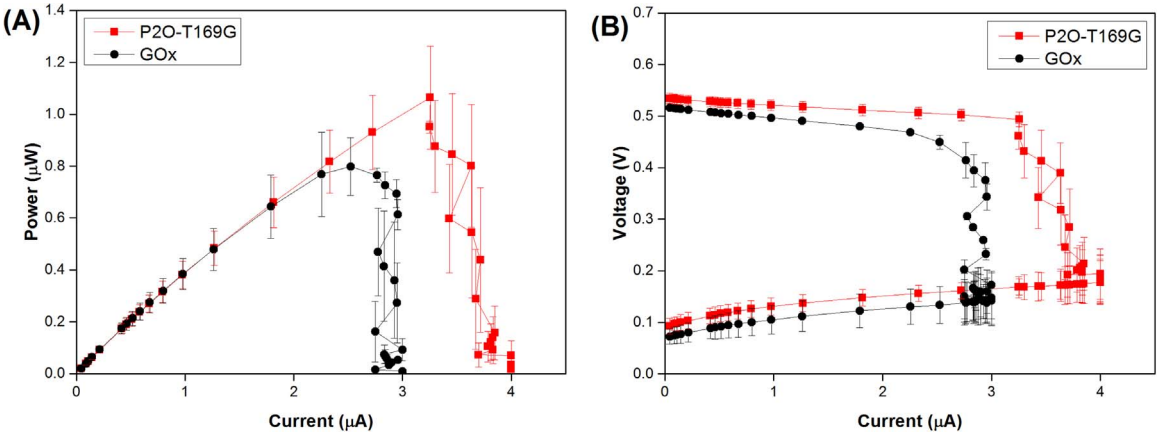

Fig. 5. (A) Power, (B) anode and cathode potentials generated by the EnFCs with P2O-T169G and GOx as anode biocatalyst and BOD as cathode biocatalyst operating at batch mode in a glass cell containing aerated solutions of 5.5 mM glucose in 0.1 M PBS at pH 7. Electrode model: DRP-C110, surface area: 0.126 cm^2. Error bars are sample standard deviations (n = 2 samples).

Fig. 7). This may be due to the fact that when immobilised on Fc-Nafion-MWCNTs carbon SPE system, specific interaction of GOx with D-glucose is different from that of free enzyme form while the immobilised or free P2O-T169G react with D-glucose similarly. The conserved active sites residues of P2O-T169G contains the conserved His/Asn pair whereas GOx has the conserved His/His pair. The difference in key catalytic residues (His in GOx vs Asn in P2O-T169G) may cause these two enzymes to interact with D-glucose differently when immobilised on Fc-Nafion-MWCNTs carbon SPE system.

3.3. Stability of enzyme electrodes modified with Fc-Nafion-MWCNTs

Stability is an important parameter especially for systems that might require continuous operation such as EnFCs and biosensors. Fig. 4 demonstrates the difference in current density values for (A) short term and (B) 12 h operation upon addition of glucose. It can be seen from Fig. 4(A) that after each consecutive glucose addition, GOx showed higher spikes in current density following by a sharp decrease. P2O-T169G, on the other hand, the current density showed smaller spikes following by consistent and stable values for consecutive glucose additions. Although this behaviour of GOx provided higher currents initially, the currents were lower than what it achieved for P2O-T169G at the end of each 10-min period.

CA experiments in aerated solution were also conducted for 12 h to compare the stability of the enzymes (Fig. 4(B)). The duration of 12 h was chosen based on the performance of the enzymes, defined as the time when the current drops at least more than 50% from their initial readings. GOx, despite having more than 5-fold higher current response than P2O-T169G initially (initial current around 55 μA and 10 μA for GOx and P2O-T169G respectively), showed almost no catalytic activity (around 0.1 μA) after 12 h of operation in 4 mM glucose, with a sharp decrease of 90% in the current within the first hour of operation. P2O-T169G showed greater performance stability than GOx because it could maintain > 70% of its initial current during the first hour and continue with just a further 30% loss over the next 10 h (final current after 12 h is around 4 μA, Fig. 4(B) inset). The initial current loss within the first hour for both of the enzymes might be related to the decrease of enzyme activity while the later activity loss might be due to combination of the glucose and activity depletion. The film stability is also another aspect that can affect the general performance of the electrodes. These results obtained from CA experiments for 12 h suggest that P2O-T169G can provide more stable current than GOx under the same conditions. This is an important finding for EnFC research as the stability of the enzymes is one of the major problems in this field.

3.4. Fuel cell performance

3.4.1. Fuel cell tests with SPEs

Comparative fuel cell tests with P2O-T169G and GOx were conducted using SPE prepared as described in 2.3.2. Fig. 5 shows the comparison between EnFCs constructed using P2O-T169G and GOx as anode biocatalyst and BOD as cathode biocatalyst in terms of power

and anode-cathode potentials.

Initially, EnFCs showed similar open circuit voltage (OCV) of 0.442 V and 0.444 V for P2O-T169G and GOx, respectively. P2O-T169G showed ca. 25% more power output than GOx with a maximum power value of 1.06 μW (8.45 μW cm^{-2}) in 5.5 mM aerated glucose solution for GOx: 0.8 μW (6.34 μW cm^{-2}). As expected from a system operating at batch mode, EnFCs were limited by the cathode performance due to limited oxygen present in solution demonstrated by rapid decrease of cathode potentials when reaching limiting current values of 3.26 μA (25. 87 μA cm^{-2}) and 2.52 μA (20 μA cm^{-2}) for P2O-T169G and GOx, respectively. Higher limiting current value suggests that the contribution of P2O-T169G enzyme into the bio-electrochemical reaction might be greater than GOx as it was indicated similarly in another study (Halámková et al., 2012).

Fig. 5(B) shows that the anodic currents are in the same range for both enzymes however the cathode used in EnFC with GOx decreased rapidly at lower current although the initial cathode performance was similar for both EnFCs. This might be because of a possible competition between GOx anode and BOD cathode over utilising O_2 in the solution. As O_2 is the natural electron acceptor for GOx, it will be used at the anode to produce H_2O_2 which can affect the cathode performance in two possible ways. It can be limiting the reduction of O_2 at the cathode as substantially consumed at the anode especially at higher loads when the reaction rate for the oxidation of glucose is relatively high. Alternatively, it can be decreasing the activity of the cathodic enzyme as it can be seen from Fig. 3(C) and (D) that there is no significant difference between air and nitrogen saturated solution results for P2O-T169G and GOx. It suggests that in this case cathode might be highly affected by the presence of peroxidase, which is known to reduce the activity of bilirubin oxidase (Milton et al., 2014). Either way, the performance of EnFC with GOx would be decreased in the presence of O_2. P2O, on other hand, performed better suggesting less activity towards oxygen in parallel with half-cell experiments. This is an important outcome regarding to the use of P2O-T169G in EnFCs so that it could be utilised in different designs such as air-breathing cells where sufficient O_2 can be supplied to the cathode without significant anodic performance loss.

3.4.2. Fuel cell tests with gas-diffusion CPEs

Fig. 6(A) shows the polarisation curve for air-breathing EnFC. The air-breathing EnFC showed an OCV value of 0.558 V which is ~ 26% more of that observed when batch system was used. Anode and cathode potentials were also measured as 0.019 ± 0.035 and 0.524 ± 0.014 V, respectively. The EnFC reached a maximum power value of 52.7 μW and power density value of 29.8 μW cm^{-2} which is 3.4-fold higher than it was in the batch system. Significant improvement was achieved for limiting current reaching 0.14 mA (0.08 mA cm^{-2}) which is 3-fold higher than it was obtained from the batch system. Since the enzyme amount used for immobilisation reaction was kept the same per surface area for SPEs and CPEs (*ca.* 0.16 mg cm^{-2}), more enzyme might be involved in the bio-electrochemical reactions assuming immobilisation was occurred at the same yield.

Another important aspect for the air-breathing EnFC can be seen in Fig. 6(B). The limitation of the EnFC was switched from cathode to anode when air-breathing cathode is implemented suggesting improved cathode performance due to sufficient O_2 provided. These analyses show that the oxygen concentration is highly important for the EnFC performance and oxygen resistant nature of P2O-T169G combined with oxygen rich cathode resulting high OCP and power output values. Fig. 6(C) demonstrates the stability of the air breathing EnFC under 4 kΩ external load showing the potential values of the cell and the percentage power loss for 3 weeks. A continuous feeding system using a peristaltic pump operating at a flow rate of 0.3 mL min^{-1} was used to have better perspective for stability of the EnFC. Anode and cathode potentials were also recorded individually to have a better view on the

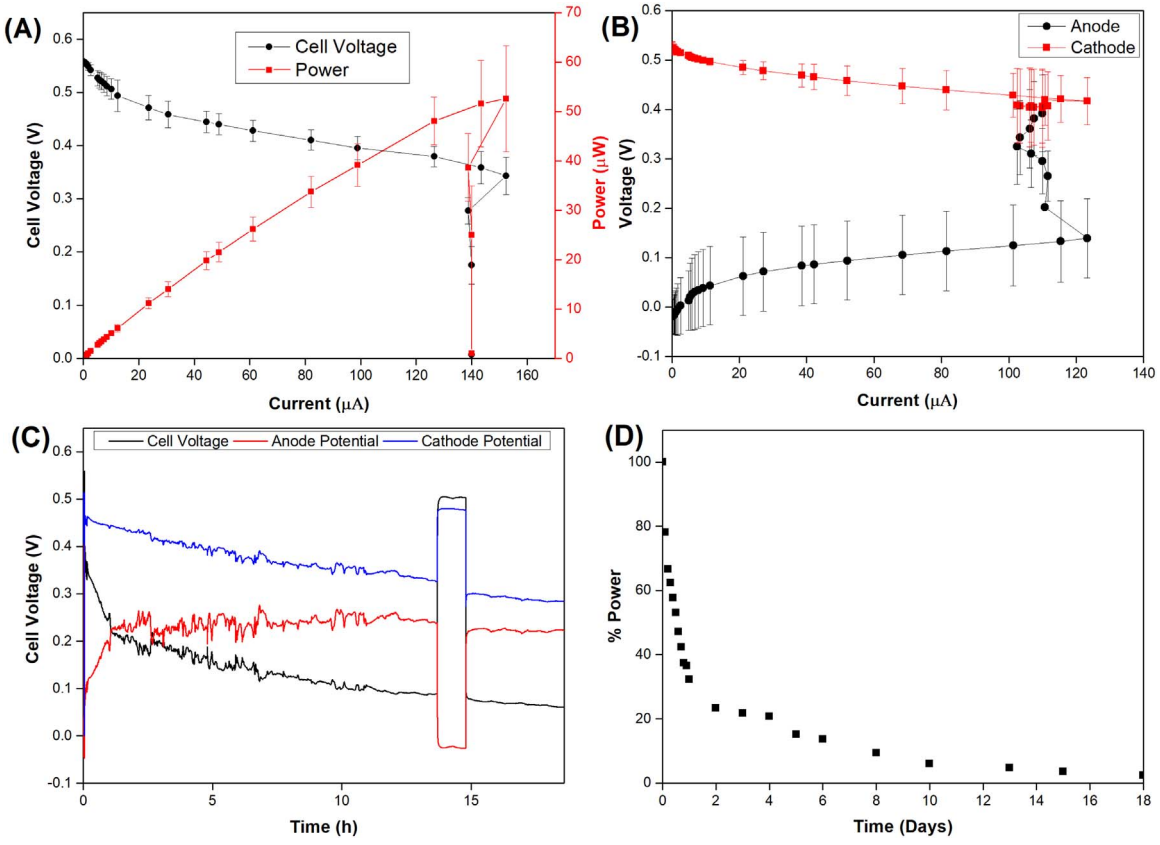

Fig. 6. (A) EnFC polarisation curve, (B) anode and cathode potentials, (C) and (D) stability measurements of the EnFC with P2O-T169G and BOD as anode and cathode respectively. Electrode model: Gas diffusion carbon paper, surface area: 1.77 cm^2. Error bars are sample standard deviations (n = 2 samples).

individual performance of the anode and cathode. The cell voltage showed a consistent decay during the first 24 h (down to ~ 32% capacity) and stabilized for the following 2 days (~ 23 and ~ 21% capacity on 2nd and 3rd day respectively) resulting an average power density value of a 5.3 μW cm^{-2}. The cell voltage then exponentially decayed for the next two weeks of operation reaching a final value of 60 mV with a power density value of a 0.57 μW cm^{-2}. During the 13th day of the operation, the load on the cell was removed and left at OCP for 24 h. It was intended to observe the behaviour of the EnFC during OCP operation and re-applying load. It was found out that after the resting period the cell was maintained the cell voltage from where it was left. This indicates that the decrease in cell voltage strongly depended of the enzyme activities.

The anode and cathode potentials also suggest that the overall cell performance was limited by anode especially during the first week of the operation. This is similar with the findings obtained from polarisation experiments. The reason for the initial decay might be due to denaturation and/or inactivation of the enzyme at the anode during a week of operation (Wieckowski, 2009). The cathode also showed decreasing voltage characteristics accordingly with anode.

Furthermore, the reason why the sharp decay in the first 24 h following by moderate decrease in the next few days might be also because of the external load chosen as it was rather closer to the maximum current density of the EnFC. Selecting the external resistance that is associated with the maximum sustainable power is very difficult as the rate of the charge transfer at the current limiting electrode or the potential across the fuel cell cannot be controlled externally (Menicucci et al., 2006). High instantaneous electric currents might be achieved which results higher than the maximum sustainable rate of charge transfer from the current limiting electrode, in this case, the anode. As a result, more studies would be carried out regarding to determining the optimum external load for sustainable power production. Cathode potential, on the other hand, was only decreased by 10% during 3 days of operation.

In the case of co-immobilizing GOx and Fc on the electrodes, the power density obtained in this study is ~ 3-fold higher than that where GOx and Fc were directly crosslinked on the electrode without using nanomaterials (13 μW cm^{-2}) (Shim et al., 2011) and where Fc, MWCNTs and chitosan were employed on the electrode (13 μW cm^{-2}) (Park et al., 2011). Furthermore, it is ~ 2-fold higher than the reported values (15.8 μW cm^{-2}) where Fc was used with carbon nanocomposite materials (Zhou et al., 2007) and similar to where graphene nano-sheets were used (24.3 μW cm^{-2}) (Liu et al., 2010), however the EnFC was tested in 100 mM glucose solution which is a lot more than 5.5 mM used in present work. The performance of the EnFC in this study was also showed power densities in the same range with that in which Fc is used as a mediator at the anode incorporation with Nafion and MWCNTs by (Tan et al., 2010). However, their fuel cell lost 94% of its initial performance after 5 h of operation at pH 5. The first demonstration of P2O enzyme in EnFCs was reported by Kwon et al. showing a power density of 40.7 μW cm^{-2} (Kwon et al., 2014). Recently, Kim et al. also reported an EnFC using enzyme precipitated coating method to immobilise P2O reaching a power density value of 53 μW cm^{-2} (Kim et al., 2017). However, both of these systems are not fully enzymatic as they utilise platinum as the cathode catalyst. Furthermore, they use a redox mediator in solutions. In comparison, this work represents a fully enzymatic and membraneless EnFC system where no dissolved mediators in sample solution used, and the power densities reached the same range of these studies.

4. Conclusions

In conclusion, a simple, effective and biocompatible immobilisation method was successfully applied to construct EnFCs with P2O-T169G. To the authors best of knowledge, this is one of the most extensive demonstration of the use of a P2O-based enzyme for EnFC applications in literature and the first-time demonstration of electrochemical glucose oxidation by an oxygen resistant variant of P2O enzyme. Based on the results obtained, P2O-T169G showed promising results in spite of its lower enzyme activity, by virtue of its stability, glucose affinity and performance as anode biocatalyst in an air-breathing EnFC reaching power density values of 29.8 ± 6.1 μW cm^{-2}. This power value is very competitive with the systems in literature where P2O is used with platinum cathode (non-enzymatic). Furthermore, P2O-T169G shows better stability and 25% more power output than widely used GOx as anode biocatalyst. Oxygen resistant P2O is a promising candidate for EnFCs using sugars as fuels.

Acknowledgements

Dr. Samet Şahin would like to thank the Turkish Government for the support during his Ph.D. study at Newcastle University. Dr. Eileen Hao Yu thank EPSRC Supergen Biological fuel cell (EP/H0194801) for funding. We thank The Thailand Research Fund Grants RTA5980001 (to P.C.), MRG6080234 (to T.W.), Royal Golden Jubilee Scholarship PHD/0172/2556 (to L.C.) for research support. We also thank Vidyasirimedhi Institute of Science and Technology (VISTEC) for their support.

Appendix A. Supplementary material

Supplementary data associated with this article can be found in the online version at http://dx.doi.org/10.1016/j.bios.2018.01.065.

References

Abdulbari, H.A., Basheer, E.A.M., 2017. ChemBioEng Rev. 4 (2), 92–105.
Bard, A.J., Faulkner, L.R., Leddy, J., Zoski, C.G., 1980. Wiley New York.
Chen, M., Wei, X., Qian, H., Diao, G., 2011. Mater. Sci. Eng.: C 31 (7), 1271–1277.
Chinnadayyala, S.R., Kakoti, A., Santhosh, M., Goswami, P., 2014. Biosens. Bioelectron. 55, 120–126.
Dai, H., 2002. Acc. Chem. Res. 35 (12), 1035–1044.
Dey, R.S., Raj, C.R., 2010. J. Phys. Chem. C 114 (49), 21427–21433.
Dong, S., Wang, B., Liu, B., 1992. Biosens. Bioelectron. 7 (3), 215–222.
Dougherty, M.J., Tran, H.M., Stavila, V., Knierim, B., George, A., Auer, M., Adams, P.D., Hadi, M.Z., 2014. PLoS One 9 (6), e100836.
Filik, H., A Avan, A., Aydar, S., 2015. Curr. Nanosci. 11 (6), 784–791.
Ghosh, T., Sarkar, P., Turner, A.P.F., 2015. Bioelectrochemistry 102 (Suppl. C), S1–S9.
Güven, G., Şahin, S., Güven, A., Yu, E.H., 2016. Front. Energy Res. 4, 4.
Halámková, L., Halámek, J., Bocharova, V., Szczupak, A., Alfonta, L., Katz, E., 2012. J. Am. Chem. Soc. 134 (11), 5040–5043.
Harkness, J.K., Murphy, O.J., Hitchens, G.D., 1993. J. Electroanal. Chem. 357 (1), 261–272.
Heller, A., 2004. Phys. Chem. Chem. Phys. 6 (2), 209–216.
Ivanov, I., Vidaković-Koch, T., Sundmacher, K., 2010. Energies 3 (4), 803.
Jönsson-Niedziolka, M., Kaminska, A., Opallo, M., 2010. Electrochim. Acta 55 (28), 8744–8750.
Kang, J., Hussain, A.T., Catt, M., Trenell, M., Haggett, B., Yu, E.H., 2014. Sens. Actuators B: Chem. 190, 535–541.
Kim, J.H., Hong, S.G., Wee, Y., Hu, S., Kwon, Y., Ha, S., Kim, J., 2017. Biosens. Bioelectron. 87, 365–372.
Kim, S.B., Kim, D.S., Yang, J.H., Lee, J., Kim, S.W., 2016. Enzym. Microb. Technol. 85 (Suppl. C), S32–S37.
Krishnan, S., Armstrong, F.A., 2012. Chem. Sci. 3 (4), 1015–1023.
Kwon, K.Y., Kim, J.H., Youn, J., Jeon, C., Lee, J., Hyeon, T., Park, H.G., Chang, H.N., Kwon, Y., Ha, S., 2014. Electroanalysis 26 (10), 2075–2079.
Lidén, H., Volc, J., Marko-Varga, G., Gorton, L., 1998. Electroanalysis 10 (4), 223–230.
Liu, C., Alwarappan, S., Chen, Z., Kong, X., Li, C.-Z., 2010. Biosens. Bioelectron. 25 (7), 1829–1833.
MacVittie, K., Halamek, J., Halamkova, L., Southcott, M., Jemison, W.D., Lobel, R., Katz, E., 2013. Energy Environ. Sci. 6 (1), 81–86.
Mani, V., Devadas, B., Chen, S.-M., 2013. Biosens. Bioelectron. 41, 309–315.
Menicucci, J., Beyenal, H., Marsili, E., Veluchamy, Demir, G., Lewandowski, Z., 2006. Environ. Sci. Technol. 40 (3), 1062–1068.
Meredith, M.T., Kao, D.-Y., Hickey, D., Schmidtke, D.W., Glatzhofer, D.T., 2011. J. Electrochem. Soc. 158 (2), B166–B174.
Milton, R.D., Giroud, F., Thumser, A.E., Minteer, S.D., Slade, R.C.T., 2014. Chem. Commun. 50 (1), 94–96.
Odaci, D., Telefoncu, A., Timur, S., 2008. Sens. Actuators B: Chem. 132 (1), 159–165.
Ozdemir, C., Yeni, F., Odaci, D., Timur, S., 2010. Food Chem. 119 (1), 380–385.
Park, H.J., Won, K., Lee, S.Y., Kim, J.H., Kim, W.-J., Lee, D.S., Yoon, H.H., 2011. Mol. Cryst. Liq. Cryst. 539 (1), 238/[578]–246/[586].

Pitsawong, W., Sucharitakul, J., Prongjit, M., Tan, T.-C., Spadiut, O., Haltrich, D., Divne, C., Chaiyen, P., 2010. J. Biol. Chem. 285 (13), 9697–9705.
Rasmussen, M., Abdellaoui, S., Minteer, S.D., 2016. Biosens. Bioelectron. 76, 91–102.
Rathee, K., Dhull, V., Dhull, R., Singh, S., 2016. Biochem. Biophys. Rep. 5, 35–54.
Sahin, S., Wongnateb, T., Chaiyenb, P., Yu, E.H., 2014. Chem. Eng. Trans. 41.
Saleem, M., Yu, H., Wang, L., Zain ul, A., Khalid, H., Akram, M., Abbasi, N.M., Huang, J., 2015. Anal. Chim. Acta 876 (Suppl. C), S9–S25.
Salek-Maghsoudi, A., Vakhshiteh, F., Torabi, R., Hassani, S., Ganjali, M.R., Norouzi, P., Hosseini, M., Abdollahi, M., 2018. Biosens. Bioelectron. 99 (Suppl. C), S122–S135.
Schievano, A., Pepe Sciarria, T., Vanbroekhoven, K., De Wever, H., Puig, S., Andersen, S.J., Rabaey, K., Pant, D., 2016. Trends Biotechnol. 34 (11), 866–878.
Scholz, F., 2010. Springer. pp. 11–31.
Shim, J., Kim, G.-Y., Moon, S.-H., 2011. J. Electroanal. Chem. 653 (1), 14–20.
Smart, S.K., Cassady, A.I., Lu, G.Q., Martin, D.J., 2006. Carbon 44 (6), 1034–1047.
Spadiut, O., Brugger, D., Coman, V., Haltrich, D., Gorton, L., 2010. Electroanalysis 22 (7–8), 813–820.
Stepnicka, P., 2008. John Wiley & Sons.
Szczupak, A., Halamek, J., Halamkova, L., Bocharova, V., Alfonta, L., Katz, E., 2012. Energy Environ. Sci. 5 (10), 8891–8895.
Tan, Y., Deng, W., Li, Y., Huang, Z., Meng, Y., Xie, Q., Ma, M., Yao, S., 2010. J. Phys. Chem. B 114 (15), 5016–5024.
Tasca, F., Timur, S., Ludwig, R., Haltrich, D., Volc, J., Antiochia, R., Gorton, L., 2007. Electroanalysis 19 (2–3), 294–302.
Timur, S., Yigzaw, Y., Gorton, L., 2006. Sens. Actuators B: Chem. 113 (2), 684–691.
Tran, T.O., Lammert, E.G., Chen, J., Merchant, S.A., Brunski, D.B., Keay, J.C., Johnson, M.B., Glatzhofer, D.T., Schmidtke, D.W., 2011. Langmuir 27 (10), 6201–6210.
Vaillancourt, M., Wei Chen, J., Fortier, G., Bélanger, D., 1999. Electroanalysis 11 (1), 23–31.
Wieckowski, A., 2009. John Wiley & Sons.
Willner, I., Yan, Y.M., Willner, B., Tel-Vered, R., 2009. Fuel Cells 9 (1), 7–24.
Wilson, R., Turner, A.P.F., 1992. Biosens. Bioelectron. 7 (3), 165–185.
Wongnate, T., Sucharitakul, J., Chaiyen, P., 2011. ChemBioChem 12 (17), 2577–2586.
Wongnate, T., Surawatanawong, P., Visitsatthawong, S., Sucharitakul, J., Scrutton, N.S., Chaiyen, P., 2014. J. Am. Chem. Soc. 136 (1), 241–253.
Yabuuchi, M., Masuda, M., Katoh, K., Nakamura, T., Akanuma, H., 1989. Clin. Chem. 35 (10), 2039–2043.
Yang, X., Hua, L., Gong, H., Tan, S.N., 2003. Anal. Chim. Acta 478 (1), 67–75.
Yu, E.H., Scott, K., 2010. Energies 3 (1), 23.
Zafar, M.N., Tasca, F., Boland, S., Kujawa, M., Patel, I., Peterbauer, C.K., Leech, D., Gorton, L., 2010. Bioelectrochemistry 80 (1), 38–42.
Zhou, Q., Xie, Q., Fu, Y., Su, Z., Jia, Xe, Yao, S., 2007. J. Phys. Chem. B 111 (38), 11276–11284.